Magnetic Resonance in Medicine 44:867–872 (2000)

High-Resolution MRI Characterization of Human Thrombus Using a Novel Fibrin-Targeted Paramagnetic Nanoparticle Contrast Agent

Xin Yu,[1*] Sheng-Kwei Song,[2] Junjie Chen,[3] Michael J. Scott,[1] Ralph J. Fuhrhop,[1] Christopher S. Hall,[1] Patrick J. Gaffney,[4] Samuel A. Wickline,[1] and Gregory M. Lanza[1]

In this study, the sensitivity of a novel fibrin-targeted contrast agent for fibrin detection was defined in vitro on human thrombus. The contrast agent was a lipid-encapsulated perfluorocarbon nanoparticle with numerous Gd-DTPA complexes incorporated into the outer surface. After binding to fibrin clots, scanning electron microscopy of treated clots revealed dense accumulation of nanoparticles on the clot surfaces. Fibrin clots with sizes ranging from 0.5–7.0 mm were imaged at 4.7 T with or without treatment with the targeted contrast agent. Regardless of sizes, untreated clots were not detectable by T_1-weighted MRI, while targeted contrast agent dramatically improved the detectability of all clots. Decreases in T_1 and T_2 relaxation times (20–40%) were measured relative to the surrounding media and the control clots. These results suggest the potential for sensitive and specific detection of microthrombi that form on the intimal surfaces of unstable atherosclerotic plaque. Magn Reson Med 44:867–872, 2000. © 2000 Wiley-Liss, Inc.

Key words: molecular imaging; MRI; gadolinium-DTPA; nanoparticles; fibrin

Atherosclerotic plaque rupture precipitates thrombus formation, which can progress to myocardial infarction and stroke. The quest to identify "vulnerable plaques" has been one of the most active areas in cardiovascular research. Conventional imaging methods, such as contrast angiography and Doppler velocity waveform analysis, have focused on detecting flow-limiting luminal stenosis without inference of artery wall thickness or lesion structure. However, remodeled vessels can maintain nearly normal lumen cross-sectional area despite the presence of significant atherosclerotic disease (1). Furthermore, recent basic and clinical research findings have challenged the emphasis on luminal stenosis in staging atherosclerosis, as plaque rupture and subsequent acute myocardial infarction have been shown to occur more often in vessels with only mild-to-moderate luminal stenosis (2,3). These findings suggest the need for new approaches that extend the precision and accuracy of current methods, as well as define vulnerable lesions in patients who are at high risk for thrombotic events. Such novel approaches would directly characterize biological activity of atherosclerotic plaques and assess their propensity for rupture and clinical thrombotic events.

MRI is a promising imaging modality that permits noninvasive vascular imaging with sub-millimeter resolution and high tissue contrast. Its multi-parametric feature allows a wide range of image contrasts (e.g., proton density weighted, T_1 or T_2 weighted, diffusion weighted, etc.), making it possible to characterize directly the atherosclerotic lesions instead of luminal cross-section. MRI has been applied to imaging and spectroscopy of ex vivo and in vivo atherosclerotic plaques in both animals and human (4–7). With increased image resolution and contrast between atherosclerotic plaque and vessel wall, these techniques provide accurate morphological measurements of atherosclerotic lesions. However, they do not supply adequate information about the biological activity of atherosclerotic plaques and their potential for rupture.

Molecular imaging with highly selective ligand-targeted contrast agents is emerging as a new tool for the sensitive and specific detection of unique cellular processes associated with a disease (8). We have previously reported the development of a novel, site-targeted paramagnetic contrast agent and its applications in molecular imaging of human thrombus (9) and molecular markers specific for angiogenesis (10). The contrast agent is a lipid-encapsulated perfluorocarbon nanoparticle which incorporates tens of thousands of Gd-DTPA complexes on its lipid surface. In this study, we determined the extent to which fibrin-targeted nanoparticles could enhance T_1- and T_2-weighted MR images of small fibrin-rich clots. An in vitro model of human thrombus was developed, and the T_1 and T_2 relaxation changes induced by the bound paramagnetic nanoparticles were characterized on a 4.7 T magnet. Our results demonstrate that the very large payload of gadolinium brought to each targeted fibrin epitope markedly enhances the potential for detection of microthrombi deposits on diseased intimal surfaces. Such an approach is expected to permit sensitive and specific early diagnosis of the clinically silent microfissuring that presages a ruptured atherosclerotic plaque.

METHODS

Preparation of Contrast Agent

The targeted MRI contrast agent was produced by incorporating a biotinylated phospholipid into the outer lipid monolayer of a perfluorocarbon nanoparticle, as described previously (9). Briefly, the nanoparticles were comprised of perfluorodichlorooctane (PFDCO) (40% v/v) (Minnesota

[1]Department of Medicine, Cardiovascular Division, Barnes-Jewish Hospital, Washington University School of Medicine, St. Louis, Missouri.

[2]Department of Chemistry, Washington University School of Medicine, St. Louis, Missouri.

[3]Department of Biomedical Engineering, Washington University, St. Louis, Missouri.

[4]Department of Surgery, St. Thomas's Hospital, London, UK.

Grant sponsor: NIH; Grant number: R01 HL-59865; Grant sponsor: Barnes-Jewish Hospital Foundation; Grant number: 5404-01; Grant sponsor: ACC/Searle.

*Correspondence to: Xin Yu, Sc.D., Campus Box 8086, 660 South Euclid Avenue, St. Louis, MO 63110. E-mail: xin@cvu.wustl.edu

Received 6 June 2000; revised 1 August 2000; accepted 1 August 2000.

© 2000 Wiley-Liss, Inc.

Manufacturing and Mining, St. Paul, MN), safflower oil (2.0% w/v), a surfactant co-mixture (2.0% w/v), and glycerin (1.7% w/v). The surfactant co-mixture of lecithin (Pharmacia Inc., Clayton, NC), cholesterol (Sigma Chemical Co., St. Louis, MO), Gd-DTPA-BOA (Gateway Specialty Chemicals, St. Louis, MO), and biotinylated phosphatidylethanolamine was dissolved in chloroform, evaporated under reduced pressure, dried in a 50°C vacuum oven, and dispersed into water by sonication, resulting in a liposome suspension. The suspension was transferred into a blender cup (Dynamics Corporation of America, New Hartford, CT) with PFDCO, safflower oil, and distilled, deionized water and continuously processed at 20,000 PSI for 4 min with an S110 Microfluidics emulsifier (Microfluidics, Newton, MA). Particle sizes were approximately 210 nm in diameter, as determined at 37°C with a laser light scatter submicron particle size analyzer (Malvern Instruments, Malvern, Worcestershire, UK).

Preparation of Plasma Clots

Fresh frozen human plasma anticoagulated with sterile sodium citrate was obtained from the hospital blood bank. To assess the efficacy of detecting and morphologically delineating fibrin microdeposits, small clots ranging from 0.5–7 mm in diameter were formed by combining citrated plasma, 100 mmol/l calcium chloride (3:1, v/v), and 5 U thrombin (Dade Behring, Germany) onto Parafilm™ (American Can, St. Louis, MO). Clots were treated as described below and embedded in 1% agarose gel in 35-mm plastic petri dishes for MRI (n = 3/group). Additional fibrin clots were prepared to characterize T_1 and T_2 changes induced by the bound paramagnetic particles and to assess the contrast enhancement provided to T_1- and T_2-weighted MR images (n = 4/group). These cylindrical clots were formed in a 5-mm plastic tube around a 5-0 silk suture, suspended in phosphate buffered saline (PBS) in a 12 × 75 mm plastic, snap-cap tube. Similar clots without the embedded suture were prepared on nylon mesh (Midwest Scientific, St. Louis, MO) for scanning electron microscopy studies.

Application of Fibrin-Targeted Contrast

Biotinylated anti-fibrin monoclonal antibodies coupled to the paramagnetic nanoparticles through avidin-biotin interactions is a classic three-step procedure previously described by our laboratory for use with in vitro targeting experiments (9). Fibrin-rich clots were incubated with 150 μg biotinylated anti-fibrin monoclonal antibodies, NIB 1H10 or NIB 5F3 (11), in PBS for 1 hr, then rinsed with PBS to remove unbound ligand. Next, the clots were incubated for 30 min with avidin (50 μg/ml PBS). The excess avidin was then washed off with PBS, and the clots were exposed to the biotinylated paramagnetic nanoparticles (30 μL/mL PBS) for an additional 30 min. All three steps of incubation were performed at 37°C. Clots with intermediate degree of contrast agent binding were prepared by partial blockade of fibrin binding sites with pretreatment of nonbiotinylated anti-fibrin antibody for 1 hr prior to the three-step contrast targeting procedure.

MRI of Fibrin Clots

MRI of the targeted clots was performed at 4.7 T on a Varian INOVA system (Varian Associates, Palo Alto, CA). Spin-echo proton images were acquired using a 5-cm custom designed birdcage coil. Both T_1- and T_2-weighted spin-echo images were acquired. Imaging parameters for T_1-weighted images were: TR = 500 msec; TE = 13 msec; FOV = 5 × 5 cm; data matrix = 512 × 256; slice thickness = 1 mm. T_2-weighted images were acquired with TR = 8 sec, TE = 200 msec, and identical spatial parameters as T_1-weighted images. These parameters yielded an in-plane resolution of 195 × 195 μm. At the end of MRI experiments, optical images of the targeted and control clots were taken with a Kodak digital camera to provide a direct comparison of clot geometry with the MR images.

To characterize the deposition of targeted nanoparticles, T_1-weighted spin-echo imaging of clots treated with Gd-DTPA conjugated nanoparticles was also performed at higher resolution using a 1-cm birdcage coil. Imaging parameters were: TR = 500 msec; TE = 13 msec; FOV = 1.3 × 1.3 cm; data matrix = 512 × 256; slice thickness = 0.5 mm. These parameters yielded an in-plane resolution of 51 × 51 μm. To determine changes in relaxation times induced by the bound paramagnetic nanoparticles, T_1 and T_2 measurements were performed using inversion recovery and Carr-Purcell-Meiboom-Gill pulse sequences, respectively. T_1 and T_2 maps were obtained by a least-square fitting of each imaging pixel to the corresponding relaxation curve using MATLAB (The Math Works, Inc., Natick, MA).

Scanning Electron Microscopy (SEM)

Fibrin-targeted, partially-blocked, and control clots (n = 3/group) were prepared as above, fixed in 2% glutaraldehyde in PBS for 1 hr, rinsed with PBS, and post-fixed in 2% osmium tetroxide for 1 hr. The fixed and washed clots were dehydrated in ascending concentrations of ethyl alcohol, 10 min/step: 50%, 70%, 90%, and 3 × 100%, followed by three 15-min washes in hexamethyldisilazane (Electron Microscopy Sciences, Fort Worth, PA). Scanning electron microscopy was performed with a Phillips scanning electron microscope. Five random regions per clot sample were imaged from 2500× to 12000× magnification and compared for nanoparticulate binding. Representative scanning electron micrographs of each treatment group were obtained.

RESULTS

Scanning electron microscopy of native plasma clots revealed a dense network of cross-linked fibrin strands (Fig. 1A). Fibrin-targeted paramagnetic nanoparticles were observed along the clot surface attached to the dense fibrin network, literally encasing each fibrin fibril on the clot surface (Fig. 1B). Pretreatment with free anti-fibrin antibody partially blocked the binding sites available to targeted nanoparticles through competitive inhibition, and reduced the density of nanoparticles bound to the surface (Fig. 1C). Such a partial blocking of contrast agent binding provided a mechanism with which to characterize the

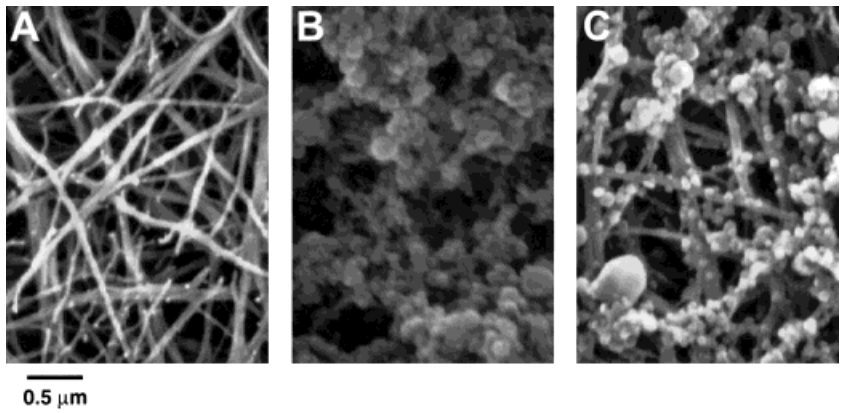

FIG. 1. Scanning electron micrographs of clots. **A:** Untreated clot. The untreated clot showed a dense network of fibrin strands. **B:** Treated clot. Clot was treated following the standard three-step incubation protocol described in the text. Fibrin strands were covered with numerous paramagnetic nanoparticles. **C:** Partially blocked clot. Clot was pretreated with non-biotinylated anti-fibrin antibody before the standard three-step treatment. As a result, a significant fraction of the fibrin binding sites was unavailable for binding to the targeted contrast agent. Therefore, the amount of paramagnetic nanoparticles was significantly reduced as compared to the treated clot.

relaxivity benefits of bound paramagnetic nanoparticles at a reduced surface density, intermediate between that of the control and unblocked clots.

Cross-sectional ^{1}H imaging of cylindrical clots suspended in PBS solution demonstrated a significant T_1 and T_2 contrast effect within the unblocked and partially-blocked fibrin-targeted clots but little inherent contrast in control clots (Fig. 2). PBS and native untreated clots had similar T_1 relaxation times: 2.21 $\pm$ 0.05 sec for PBS and 2.04 $\pm$ 0.03 sec for native clots. However, with the binding of paramagnetic nanoparticles, a significant decrease in T_1 (1.37 $\pm$ 0.28 sec) was induced on the surface of the clots (Fig. 3). Similarly, T_2 relaxation was 163 $\pm$ 4 msec and 147 $\pm$ 3 msec for PBS and native clots respectively, and was reduced to 122 $\pm$ 17 msec with the binding of paramagnetic nanoparticles. These changes in T_1 and T_2 relaxation times induced by the bound paramagnetic nanoparticles allowed excellent delineation of clots in PBS with both T_1- and T_2-weighted images (Fig. 2).

The high-resolution ^{1}H image revealed that the binding of the targeted nanoparticles was restricted to a thin layer on the clot surface (Fig. 4), as the enhanced MR signal was present within only one or two pixels ($<$ 100 μm). Exclusion of the nanoparticles from deeper aspects of these experimental fibrin-rich clots has been previously described in imaging procedures with high-frequency ultrasound (12). The restriction of the nanoparticles to surface-binding epitopes reflects the high density and tight packing of fibrin fibrils in these acellular experimental clots. In vivo, the entrapment of erythrocytes, white blood cells, and platelets within the thrombus is expected to create a porous tissue into and through which nanoparticles can more readily penetrate, as previously demonstrated in ultrasound molecular imaging applications with the use of clinical echocardiographic scanners (12). Nevertheless, despite the thin layer of contrast agent deposition, T_1- and T_2-weighted spin-echo images exhibited significant contrast enhancement at the surface of the clots due to the great abundance of Gd-DTPA complexes carried by each particle. In other words, only a single layer of nanoparticles is required to produce a significant contrast effect.

The detection of microthrombi within the microfissures of atherosclerotic plaques depends on how many nanoparticles are deposited at a given site, which reflects clot size. To better assess this question, fibrin clots as small as 0.5 mm in diameter were created and embedded in agarose gel. Optical images of these clots (Fig. 5) provided a direct morphological comparison with contrast-enhanced MR images. Untreated clots were undetectable in agarose gel

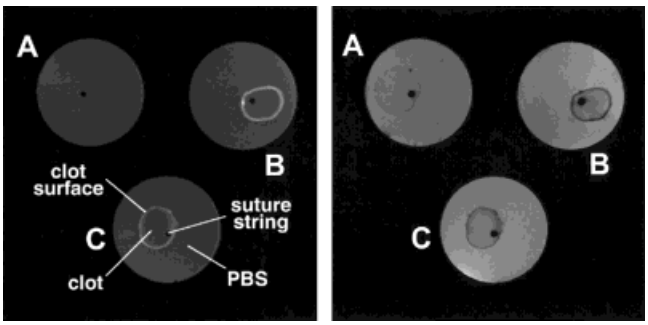

FIG. 2. Cross-sectional T_1- (left) and T_2- (right) weighted spin-echo images of cylindrical clots formed on suture strings. Clots were suspended in PBS solution and imaged with a 5-cm birdcage coil. Untreated clot (**A**) showed minimal contrast with PBS solution in both T_1- and T_2-weighted images. With the binding of contrast agent on the surfaces of the clots, both treated (**B**) and partially blocked (**C**) clots showed excellent contrast with surrounding PBS solution due to the decrease in both T_1 and T_2 relaxation times.

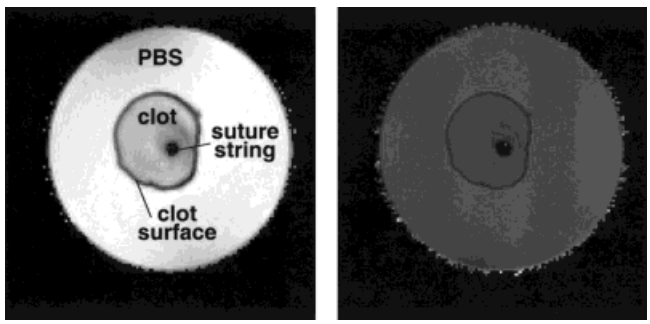

FIG. 3. T_1- (left) and T_2- (right) maps of a treated clot. Due to the high density and tight packing of fibrin strands in the clot, the binding of the contrast agent was restricted to the surface of clot. As a result, relaxation times of native or untreated clot can be determined from ROIs surrounding the suture string but excluding the surface area. T_1 and T_2 relaxation times of native clots were slightly shorter than that of PBS solution. However, the binding of contrast agent to the surface of the clot induced a 40% decrease in T_1 and a 20% decrease in T_2.

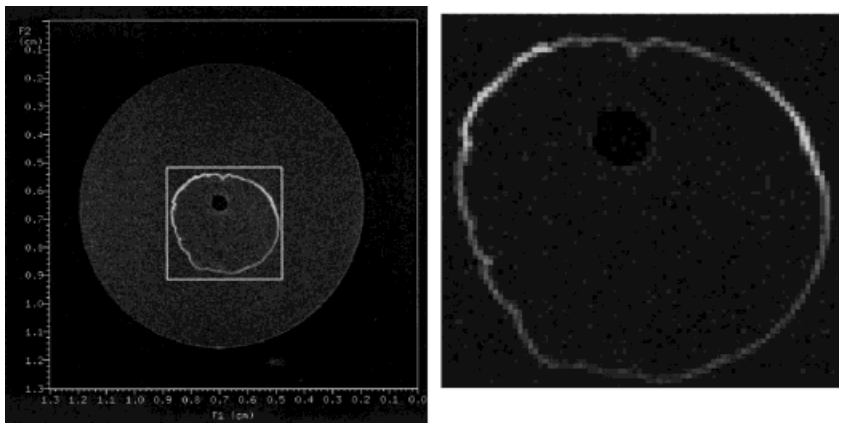

FIG. 4. High-resolution ^{1}H image of a treated clot. In-plane voxel was 51 × 51 μm. Slice thickness was 0.5 mm. The highlighted area of the clot in the original image (left panel) is shown enlarged in the right panel. It reveals that the contrast agent was deposited in a thin layer of less than 100 μm. The dramatic contrast effect with such a thin layer of contrast agent deposition demonstrates the high sensitivity of this approach, which is a result of the high Gd-DTPA payload carried by each paramagnetic nanoparticle.

by T_1-weighted MRI. However, fibrin-targeted clots were easily detected and the fine details of their geometric shapes were readily delineated for even the smallest clot (0.5 mm in diameter). In addition, all clots that were partially blocked with free anti-fibrin antibody were also sensitively detected and their geometric shapes were also sharply defined regardless of sizes. The retention of this dramatic contrast enhancement despite the marked reduction of nanoparticle deposition in the partially blocked specimens illustrates the importance of the high gadolinium payload per particle.

DISCUSSION

Accurate and sensitive detection of vulnerable atherosclerotic plaques remains a significant diagnostic challenge with great clinical relevance. Several laboratories have pursued MRI-based characterization of atherosclerotic le-

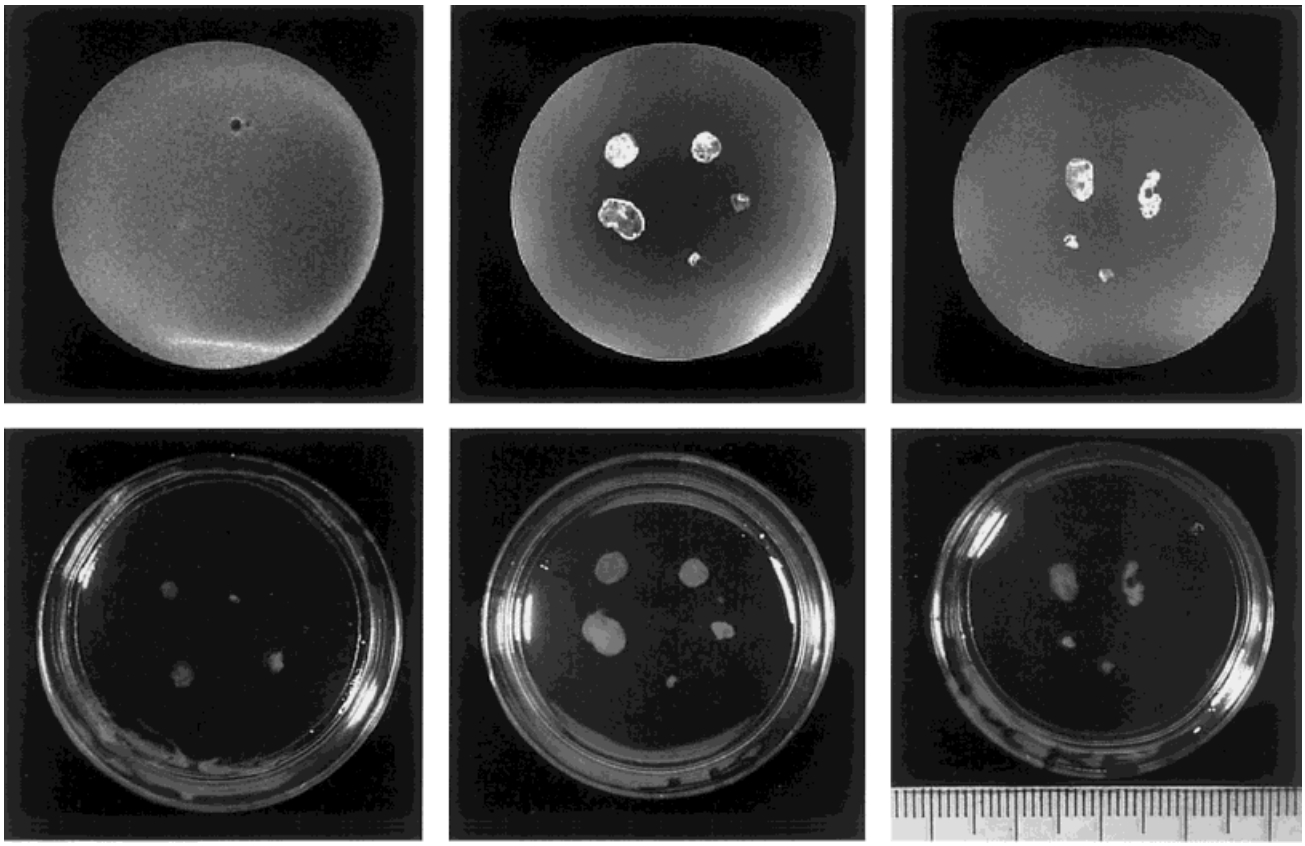

FIG. 5. T_1-weighted spin-echo images (upper panels) of clots embedded in agarose gel on a petri dish. Each small grid in the scalar bar represents 1 mm. Untreated clots (left) showed no contrast with agarose gel, while both treated (center) and partially blocked (right) clots showed excellent contrast. Direct comparison with the corresponding optical images (lower panels) indicates that MR images can also accurately delineate the morphology of the clots.

sions in an effort to estimate the propensity of plaque rupture. These tissue characterization approaches rely on defining local differences in T_1 or T_2 relaxation between lipid, fibrous, and smooth muscle components of plaques. For example, T_1-weighted images have been used to determine arterial wall area (5). T_2 contrast has been employed to discriminate atherosclerotic components such as lipid cores, fibrous caps, and calcification (13). Longitudinal monitoring of lesion progression has been reported in serial MRI experiments (4). With the use of intravascular probes or high-field magnets, imaging resolution of around 100×100 μm has been achieved, which allowed accurate determination of plaque components and the imaging of genetically engineered mice (6,7). In most of these studies, the delineation of a vulnerable plaque depends on the presence and detectability of a large, liquid lipid core, which generally favors rupture as compared with a fibrous core (14). Although these approaches may characterize certain aspects of the material properties of plaques, the definitive diagnosis of microfissuring and fibrin deposition that causes transient ischemic attacks, stroke, unstable angina, or myocardial infarction cannot be easily achieved. Accordingly, we have sought to detect the microthrombi themselves, which are the direct indicators of microscopic cracks in the collagen cap of advanced plaques that trigger thrombi (15).

Atherosclerotic plaques have been targeted with antibodies against plaque components such as proliferating smooth muscle cells (16), fibrin and fibrinogen (17,18), and extracellular matrix components such as fibronectin (19). These studies employed either radiolabeled antibodies for nuclear imaging or echogenic liposomes for ultrasonic imaging; both were limited by low image resolution. Although MRI has the advantages of offering much higher spatial resolution and simultaneous extraction of physiological and anatomic information, its application in molecular imaging has been limited by its low sensitivity. The paramagnetic nanoparticles used in this study provided a remarkable signal amplification platform that allowed sensitive detection of molecular epitopes at micrometer resolution.

The development of targeted paramagnetic contrast agents has been pursued by other laboratories and institutions for over 20 years (20). However, various complexities have contributed to the slow progress in this arena—the most important factor being inadequate paramagnetic payload, as only one to three Gd-DTPA chelates may be reasonably coupled directly to an antibody. To amplify the signal, approaches using liposomes have been employed to encapsulate larger volumes of Gd-DTPA. In early formulations, the paramagnetic chelate was sequestered internally, which yielded limited influence on protons outside of the particle and thus resulted in poor contrast enhancement (21). Coupling paramagnetic complexes to lipid anchors offers the capability of conjugating more gadolinium complexes onto the surface of liposomal particles, although at least half of the chelate complexes still typically reside within the inner membranes of the liposome bilayer (22). Multilamellar liposomes have the greatest payload capacity, but systemic clearance is accelerated and much of the paramagnetic chelates are internalized. Incorporation of polymerized lipids or polyethylene glycol-conjugated lipids provides improved liposomal half-life, although usually at the expense of targeting efficiency (23–26). Dendrimers may allow increased numbers of paramagnetic complexes to be coupled to a ligand for targeting, but their practical size limits their potential payload (27,28).

Short circulating half-life has limited the practical utility of many targeted paramagnetic formulations. Small unilaminar liposomes (50 nm) have the longest circulating half-life but carry the smallest paramagnetic payloads. Larger unilamellar liposomes have greater paramagnetic payload capacity but inadequate circulatory stability. The perfluorocarbon nanoparticles used in this study have a relatively long circulatory half-life, which permits adequate time to reach and saturate targets directly accessible to the vasculature (29).

High target avidity, i.e., multiple ligands per particle, is also critical to effective and efficient in vivo targeting. Dendrimers or similar complexes can carry large payloads of paramagnetic complexes but typically bear one or a few ligands per targeted unit. Such formulations are less likely to be properly oriented to facilitate interaction with the targeted epitope as it flows through the tissue. In comparison, perfluorocarbon nanoparticles, with tens to hundreds of ligands homogeneously distributed over the surface of each particle, experience a greater opportunity to interact and bind to one or more receptors with every circulatory pass, independent of the particle orientation. Moreover, cross-links formed by coupling the paramagnetic nanoparticle to more than one targeted epitope decrease the dissociation constant of the complex.

The degree of contrast enhancement observed in this in vitro study represents a possible benchmark for future in vivo studies. As the two antibodies used in this study are highly specific for fibrin E domain but are not cross-reactive with circulating fibrinogen (11,30), we expect this nanoparticle will only enhance contrast at the sites of fibrin deposition in vivo. Success in imaging small structures will depend largely on the quantitative deposition of nanoparticles at targeted site. We have recently reported the utility of a single-step $\alpha_v\beta_3$-targeted paramagnetic nanoparticle to localize and enhance the T_1-weighted contrast from angiogenic vasculature in rabbits (10,31). This contrast effect was easily detected within 60 min, and was maximal in less than 2 hr. In comparison, a similar study reported by Sipkins et al. (26) using $\alpha_v\beta_3$-targeted polymerized liposomes to experimental tumor angiogenesis required about 24 hr to develop a notably lower magnitude of contrast enhancement. Although highly successful in vitro, the three-step pretargeting approach using avidin-biotin interaction for binding may achieve limited success in vivo due to the high level of free biotin in circulation. Accordingly, we have recently developed an alternative approach using a "one-step system" which directly conjugates antibodies to the lipid outer layer of the nanoparticles (32). Such an approach has shown promise in preliminary in vivo studies of clot targeting with dogs in our laboratory (unpublished data).

CONCLUSION

In the present study, we have demonstrated that fibrin-targeted paramagnetic nanoparticles bound densely to fi-

brin, as visualized by scanning electron microscopy. The abundant payload of Gd-DTPA complexes provided significant enhancement of fibrin clots in vitro despite being limited to only a thin surface layer. We have shown that microdeposits of fibrin can be sensitively detected and their geometric structure clearly delineated. Future studies will extend these findings to human atherosclerotic specimens with comparisons between histology and MRI. Successful in vitro demonstration of sensitive and specific contrast enhancement of these specimens will provide impetus for further clinical evaluation. This novel, targeted MRI agent may allow sensitive early detection of unrecognized vascular pathology in high-risk patients, leading to definitive early diagnosis and the initiation of preventative therapies that could reduce the morbidity and mortality of thromboembolism.

ACKNOWLEDGMENTS

The authors thank Dr. Joseph J.H. Ackerman, Director of the Biomedical MR Laboratory at Washington University, for the technical assistance and MR resources provided by him. This work was supported by NIH grant R01 HL-59865 (S.A.W.), Barnes-Jewish Hospital Foundation grant 5404-01 (X.Y.), and ACC/Searle Career Development Award in Cardiovascular Disease (G.M.L.).

REFERENCES

1. Glagov S, Weisenberg E, Zarins CK, Stankunavicius R, Kolettis GJ. Compensatory enlargement of human atherosclerotic coronary arteries. N Engl J Med 1987;316:1371–1375.
2. Libby P. Molecular bases of the acute coronary syndromes. Circulation 1995;91:2844–2850.
3. Gutstein DE, Fuster V. Pathophysiology and clinical significance of atherosclerotic plaque rupture. Cardiovasc Res 1999;41:323–333.
4. Skinner MP, Yuan C, Mitsumori L, Hayes CE, Raines EW, Nelson JA, Ross R. Serial magnetic resonance imaging of experimental atherosclerosis detects lesion fine structure, progression and complications in vivo. Nat Med 1995;1:69–73.
5. Yuan C, Beach KW, Smith LH, Hatsukami TS. Measurement of atherosclerotic carotid plaque size in vivo using high resolution magnetic resonance imaging. Circulation 1998;98:2666–2671.
6. Fayad ZA, Fallon JT, Shinnar M, Wehrli S, Dansky HM, Poon M, Badimon JJ, Charlton SA, Fisher EA, Breslow JL, Fuster V. Noninvasive in vivo high-resolution magnetic resonance imaging of atherosclerotic lesions in genetically engineered mice. Circulation 1998;98:1541–1547.
7. Zimmermann-Paul GG, Quick HH, Vogt P, von Schulthess GK, Kling D, Debatin JF. High-resolution intravascular magnetic resonance imaging: monitoring of plaque formation in heritable hyperlipidemic rabbits. Circulation 1999;99:1054–1061.
8. Weissleder R. Molecular imaging: exploring the next frontier. Radiology 1999;212:609–614.
9. Lanza GM, Lorenz CH, Fischer SE, Scott MJ, Cacheris WP, Kaufmann RJ, Gaffney PJ, Wickline SA. Enhanced detection of thrombi with a novel fibrin-targeted magnetic resonance imaging agent. Acad Radiol 1998;5:S173–176.
10. Anderson SA, Rader RK, Westlin WF, Null C, Lanza GM, Wickline SA, Kotyk JJ. Rapid magnetic resonance contrast enhancement of neovascular with $\alpha_v\beta_3$ targeted nanoparticles. Magn Reson Med 2000;44:433–439.
11. Raut S, Gaffney PJ. Evaluation of the fibrin binding profile of two anti-fibrin monoclonal antibodies. Thromb Haemost 1996;76:56–64.
12. Lanza GM, Wallace KD, Scott MJ, Cacheris WP, Abendschein DR, Christy DH, Sharkey AM, Miller JG, Gaffney PJ, Wickline SA. A novel site-targeted ultrasonic contrast agent with broad biomedical application. Circulation 1996;94:3334–3340.
13. Toussaint JF, LaMuraglia GM, Southern JF, Fuster V, Kantor HL. Magnetic resonance images lipid, fibrous, calcified, hemorrhagic, and thrombotic components of human atherosclerosis in vivo. Circulation 1996;94:932–938.
14. Rabbani R, Topol EJ. Strategies to achieve coronary arterial plaque stabilization. Cardiovasc Res 1999;41:402–417.
15. Constantinides P. Cause of thrombosis in human atherosclerotic arteries. Am J Cardiol 1990;66:37G–40G.
16. Narula J, Petrov A, Pak KY, Ditlow C, Chen F, Khaw BA. Noninvasive detection of atherosclerotic lesions by 99mTc-based immunoscintigraphic targeting of proliferating smooth muscle cells. Chest 1997;111:1684–1690.
17. Mettinger KL, Larsson S, Ericson K, Casseborn S. Detection of atherosclerotic plaques in carotid arteries by the use of 123I-fibrinogen. Lancet 1978;1:242–244.
18. Demos SM, Onyuksel H, Gilbert J, Roth SI, Kane B, Jungblut P, Pinto JV, McPherson DD, Klegerman ME. In vitro targeting of antibody-conjugated echogenic liposomes for site-specific ultrasonic image enhancement. J Pharm Sci 1997;86:167–171.
19. Uehara A, Isaka Y, Hashikawa K, Kimura K, Kozuka T, Kamada T, Etani H, Yoneda S, Imaizumi M. Iodine-131-labeled fibronectin: potential agent for imaging atherosclerotic lesion and thrombus. J Nucl Med 1988;29:1264–1267.
20. Gupta H, Weissleder R. Targeted contrast agents in MR imaging. Magn Reson Imaging Clin N Am 1996;4:171–184.
21. Barsky D, Putz B, Schulten K, Magin RL. Theory of paramagnetic contrast agents in liposome systems. Magn Reson Med 1992;24:1–13.
22. Tilcock C, Ahkong QF, Koenig SH, Brown RD, Davis M, Kabalka G. The design of liposomal paramagnetic MR agents: effect of vesicle size upon the relaxivity of surface-incorporated lipophilic chelates. Magn Reson Med 1992;27:44–51.
23. Allen TM, Hansen C. Pharmacokinetics of stealth versus conventional liposomes: effect of dose. Biochim Biophys Acta 1991;1068:133–141.
24. Allen TM, Hansen C, Martin F, Redemann C, Yau-Young A. Liposomes containing synthetic lipid derivatives of poly(ethylene glycol) show prolonged circulation half-lives in vivo. Biochim Biophys Acta 1991;1066:29–36.
25. Storrs RW, Tropper FD, Li HY, Song CK, Sipkins DA, Kuniyoshi JK, Bednarski MD, Strauss H, Li KC. Paramagnetic polymerized liposomes as new recirculating MR contrast agents. J Magn Reson Imaging 1995;5:719–724.
26. Sipkins DA, Cheresh DA, Kazemi MR, Nevin LM, Bednarski MD, Li KC. Detection of tumor angiogenesis in vivo by $\alpha_v\beta_3$-targeted magnetic resonance imaging. Nat Med 1998;4:623–626.
27. Wiener EC, Brechbiel MW, Brothers H, Magin RL, Gansow OA, Tomalia DA, Lauterbur PC. Dendrimer-based metal chelates: a new class of magnetic resonance imaging contrast agents. Magn Reson Med 1994;31:1–8.
28. Bryant LH, Brechbiel MW, Wu C, Bulte JW, Herynek V, Frank JA. Synthesis and relaxometry of high-generation (G = 5, 7, 9, and 10) PAMAM dendrimer-DOTA-gadolinium chelates. J Magn Reson Imaging 1999;9:348–352.
29. Lanza GM, Trousil R, Wallace K, Abendschein DR, Scott MJ, Miller J, Gaffney PJ, Wickline SA. In vivo efficacy of fibrin targeted perfluorocarbon contrast system following intravenous injection reflects prolonged systemic half-life and persistent acoustic contrast effect. Circulation 1997;95(Suppl 1):I–457.
30. Tymkewycz PM, Creighton-Kempsford LJ, Gaffney PJ. Generation and partial characterization of five monoclonal antibodies with high affinities for fibrin. Blood Coagul Fibrinolysis 1993;4:211–221.
31. Anderson SA, Rader RK, Westlin WF, Null C, Lanza GM, Wickline SA, Kotyk JJ. Rapid, one-step antibody-targeted magnetic resonance contrast enhancement of neovascular $\alpha_v\beta_3$ epitopes using a nanoparticulate emulsion. In: Proceedings of the 7th Annual Meeting of ISMRM, Philadelphia, 1999. p 144.
32. Lanza GM, Abendschein DR, Hall CS, Marsh JN, Scott MJ, Scherrer DE, Wickline SA. Molecular imaging of stretch-induced tissue factor expression in carotid arteries with intravascular ultrasound. Invest Radiol 2000;35:227–234.